Article

Activation Enthalpies and Entropies for the Microscopic Rate Constants of Acetate-Catalyzed Isomerization of 5-Androstene-3,17-dione

Wendy J. Houck, and Ralph M. Pollack

J. Am. Chem. Soc., **2003**, 125 (34), 10206-10212• DOI: 10.1021/ja035957r • Publication Date (Web): 30 July 2003

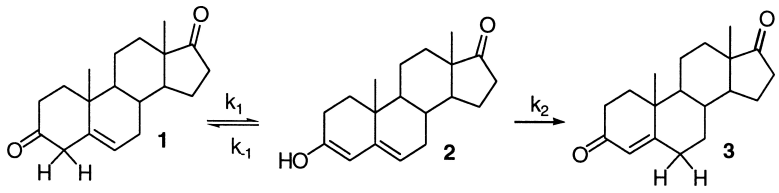

More About This Article

Additional resources and features associated with this article are available within the HTML version:

- Supporting Information
- Links to the 1 articles that cite this article, as of the time of this article download
- Access to high resolution figures
- Links to articles and content related to this article
- Copyright permission to reproduce figures and/or text from this article

View the Full Text HTML

J|A|C|S
ARTICLES
Published on Web 07/30/2003

Activation Enthalpies and Entropies for the Microscopic Rate Constants of Acetate-Catalyzed Isomerization of 5-Androstene-3,17-dione

Wendy J. Houck and Ralph M. Pollack*

Contribution from the Department of Chemistry and Biochemistry, University of Maryland, Baltimore County, 1000 Hilltop Circle, Baltimore, Maryland 21250

Received May 5, 2003; E-mail: pollack@umbc.edu

Abstract: Both acetic acid and acetate catalyze the isomerization of 5-androstene-3,17-dione (**1**) to its conjugated isomer, 4-androstene-3,17-dione (**3**), through a dienol(ate) intermediate. The temperature dependence of the overall isomerization rate constants and of the microscopic rate constants for this isomerization was determined, and the Arrhenius plots give the activation enthalpy and entropy for each step. The source of the activation energy for the overall isomerization and for each of the individual steps is predominantly enthalpic, with a moderate to low entropic penalty. Additionally, the entropy and enthalpy for the keto−enol equilibrium of **1** and dienol were determined; this equilibrium is entirely controlled by enthalpy with no entropic contribution. The relevance of these results to the mechanism of the isomerization of **1** catalyzed by the enzyme 3-oxo-Δ^5-steroid isomerase is discussed.

Introduction

Isomerizations involving enol(ate) intermediates have been extensively studied because of their simple chemistry and the occurrence of this type of reaction in the action of many important enzymes. Much effort has gone into the elucidation of the mechanisms of enzymes that catalyze this reaction, such as triosephosphate isomerase,[1−4] 4-oxalocrotonate isomerase,[5−7] and 3-oxo-Δ^5-steroid isomerase (ketosteroid isomerase, KSI).[8−14] The chemistry that occurs is of particular interest because these enzymes are able to accelerate the rate of reaction up to 15 orders of magnitude.[15,16]

The general mechanism for the nonenzymatic isomerization of β,γ-unsaturated ketones involves acid- or base-catalyzed proton abstraction from the α-carbon of the ketone to form an intermediate dienol(ate), followed by subsequent reprotonation at the γ-carbon.[17,18] An important example of this type of reaction is the isomerization of 5-androstene-3,17-dione (**1**), a substrate for KSI, to its conjugated isomer, 4-androstene-3,17-dione (**3**), shown in Scheme 1. Isomerization of **1** is catalyzed by acid,[19] hydroxide,[20] and acetate,[11] as well as KSI.[8]

Scheme 1

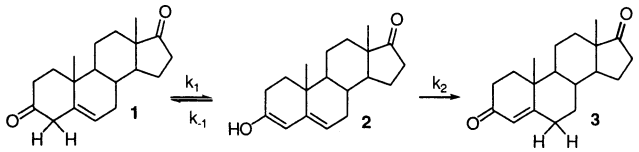

Our interest in the acetate-catalyzed isomerization of **1** is related to its use as a model for the corresponding isomerization by KSI. Acetate is a particularly good model for KSI because (1) the reaction mechanisms are quite similar, (2) KSI uses the same functional group as the active site base, Asp38, and (3) acetate and Asp38 of KSI have similar pK_a's.[21,22] Both mechanisms involve proton abstraction from C-4 by a carboxylate followed by reprotonation at C-6. Because of these similarities, acetate has served as a useful model to study the kinetics and mechanism of KSI.[9−11] We have previously determined the free-energy profile for both the KSI-catalyzed isomerization of **1**

(1) Knowles, J. R. *Philos. Trans. Biol. Sci.* **1991**, *322*, 115.
(2) Raines, R. T.; Sutton, E. L.; Straus, D. R.; Gilbert, W.; Knowles, J. R. *Biochemistry* **1986**, *25*, 7145.
(3) Hermes, J. D.; Blacklow, S. C.; Knowles, J. R. *Cold Spring Harbor Symp. Quant. Biol.* **1987**, *52*, 597.
(4) Amyes, T. L.; O'Donoghue, A. C.; Richard, J. P. *J. Am. Chem. Soc.* **2001**, *123*, 11325.
(5) Whitman, C. P. *Arch. Biochem. Biophys.* **2002**, *402*, 1.
(6) Czerwinski, R. M.; Harris, T. K.; Massiah, M. A.; Mildvan, A. S.; Whitman, C. P. *Biochemistry* **2001**, *40*, 1984.
(7) Taylor, A. B.; Czerwinski, R. M.; Johnson, W. H., Jr.; Whitman, C. P.; Hackert, M. L. *Biochemistry* **1998**, *37*, 14692.
(8) Pollack, R. M.; Thornburg, L. D.; Wu, Z. R.; Summers, M. F. *Arch. Biochem. Biophys.* **1999**, *370*, 9.
(9) Thornburg, L. D.; Goldfeder, Y. R.; Wilde, T. C.; Pollack, R. M. *J. Am. Chem. Soc.* **2001**, *123*, 9912.
(10) Hawkinson, D. C.; Eames, T. C.; Pollack, R. M. *Biochemistry* **1991**, *30*, 10849.
(11) Zeng, B.; Pollack, R. M. *J. Am. Chem. Soc.* **1991**, *113*, 3838.
(12) Zhao, Q.; Abeygunawardana, C.; Gittis, A. G.; Mildvan, A. S. *Biochemistry* **1997**, *36*, 14616.
(13) Massiah, M. A.; Abeygunawardana, C.; Gittis, A. G.; Mildvan, A. S. *Biochemistry* **1998**, *37*, 14701.
(14) Ha, N. C.; Choi, G.; Choi, K. Y.; Oh, B. H. *Curr. Opin. Struct. Biol.* **2001**, *11*, 674.
(15) Whitman, C. P.; Aird, B. A.; Gillespie, W. R.; Stolowich, N. J. *J. Am. Chem. Soc.* **1991**, *113*, 3154.
(16) Radzicka, A.; Wolfenden, R. *Science* **1995**, *267*, 90.
(17) Noyce, D. S.; Evett, M. *J. Org. Chem.* **1972**, *37*, 394.
(18) Whalen, D. L.; Weimaster, J. F.; Ross, A. M.; Radhe, R. *J. Am. Chem. Soc.* **1976**, *98*, 7319.
(19) Malhotra, S. K.; Ringold, H. J. *J. Am. Chem. Soc.* **1965**, *87*, 3228.
(20) Pollack, R. M.; Mack, J. P. G.; Eldin, S. *J. Am. Chem. Soc.* **1987**, *109*, 5048.
(21) Dean, J. A., Ed. *Lange's Handbook of Chemistry*, 13th ed.; McGraw-Hill: New York, 1985; pp 5−62.
(22) Pollack, R. M.; Bantia, S.; Bounds, P. L.; Koffman, B. M. *Biochemistry* **1986**, *25*, 1905.

10.1021/ja035957r CCC: $25.00

Table 1. Rate Constants for the Overall Isomerization of **1** to **3** Catalyzed by Acetic Acid and Acetate Ion[a]

temperature (°C)[b]	$10^5\,k_{isom}^{HOAc}$ ($M^{-1}\,s^{-1}$)	$10^5\,k_{isom}^{OAc}$ ($M^{-1}\,s^{-1}$)
10.3	0.55 ± 0.05	1.06 ± 0.05
15.2	1.0 ± 0.2	1.4 ± 0.2
20.0	1.8 ± 0.4	2.5 ± 0.4
25.0	2.2 ± 0.4	3.3 ± 0.4
29.9	3.6 ± 0.8	5.4 ± 0.8
34.7	5.0 ± 1.0	8.4 ± 1.0
39.8	5.7 ± 1.6	14.9 ± 1.6

[a] 3.3% MeOH, $\mu = 1.0$ M with NaCl. [b] Reported temperatures are ±0.1 °C.

and the corresponding acetate-catalyzed reaction at 25°.[10,11] In each case, all of the microscopic rate constants of Scheme 1 were determined. The present work extends those experiments with acetate to cover a range of temperatures. The activation enthalpies and entropies for the enolization and ketonization steps, as well as the equilibrium constants for various species of the isomerization reaction, are analyzed and discussed.

Results

Thermodynamic activation parameters for reactions can be determined through an examination of temperature-dependent kinetics according to the Arrhenius law: $\ln(k) = \ln(A) - E_a/RT$, where k is the rate constant, E_a is the activation energy related to the enthalpy of activation ($\Delta H^{\ddagger}$), R is the ideal gas constant, T is the temperature in degrees Kelvin, and A is a preexponential term related to the entropy of activation ($\Delta S^{\ddagger}$) as shown in eq 1:

$$A = (k_B T/h)e^{\Delta S/R} \qquad (1)$$

Over small temperature ranges, a plot of $\ln(k)$ vs $1/T$ is generally linear, yielding a slope that corresponds to the enthalpy of activation. From the intercept of this line, the entropy of activation can be determined. In a similar manner, by measuring equilibrium constants (K) over a range of temperatures, the enthalpies and entropies associated with these equilibria can be determined using the van't Hoff equation, $\ln(K) = -\Delta H/RT + \Delta S/R$.

Temperature Dependence of the Rate Constant for Overall Isomerization of 1 to 3 (k_{isom}). Acetate-catalyzed isomerization of **1** was monitored spectrally by observing the increase in absorbance at 248 nm due to conversion of **1** to **3** (pH = 3.7−5.3, ca. 10−40 °C). The reaction was followed for 4−5 half-lives, and progress curves were fit to a first-order exponential increase to give the observed rate constants. These rate constants were then plotted vs total acetate concentration ($[AcO^-] + [AcOH]$) to yield k_{isom}. y-Intercepts of plots of k_{isom} vs the mole fraction of acetate (m_f^{OAc}) at $m_f^{OAc} = 0$ and $m_f^{OAc} = 1$ yield the second-order rate constants for acetic acid-catalyzed isomerization of **1** (k_{isom}^{HOAc}) and acetate ion-catalyzed isomerization of **1** (k_{isom}^{OAc}), respectively (Table 1). As was previously observed in our laboratory,[11] isomerization of **1** to **3** is catalyzed by both acetic acid and acetate ion. Agreement with previously determined values at 25.0 °C is excellent (±<5%).

Arrhenius plots of $\ln k_{isom}^{OAc}$ and $\ln k_{isom}^{HOAc}$ are shown in Figure 1, with slopes corresponding to $\Delta H^{\ddagger} = 15.2 \pm 0.8$ and 13.5 ± 0.8 kcal/mol, respectively, and y-intercepts corresponding to $T\Delta S^{\ddagger} = -8.3 \pm 0.8$ and -10.3 ± 1.0 kcal/mol, respectively.

Temperature Dependence of the Rate Constant for Conversion of 1 to 2 (k_1). Proton exchange with deuterium at C-4 of **1** in D_2O was monitored by NMR in acetic acid/acetate ion buffers (pD = 4.5−5.5, ca. 13−33 °C). Peaks due to the two C-4 protons, α and β, have chemical shifts of 2.82 and 3.45 ppm, respectively.[11] These peaks were integrated relative to the C-19 methyl peak (1.2 ppm) as a function of time using FELIX 2.3 software (Biosym Technologies, San Diego, CA). The 1.2 ppm peak was normalized to 1.000 at $t = 0$ s and did not change with respect to time; thus, it serves as an internal standard. Relative integration areas for both C-4α and C-4β protons vs time were fit to a pseudo-first-order exponential decay to yield values of the rate constants for exchange of H-4α and H-4β, k_{obs}^{α} and k_{obs}^{β}, respectively. Plots of k_{obs}^{α} and k_{obs}^{β} vs the concentration of acetate are linear, with no contribution from HOAc catalysis and yield the second-order rate constants for the conversion of **1** to **2**, $k_1^{OAc}(4\alpha)$ and $k_1^{OAc}(4\beta)$, respectively (Table 2).

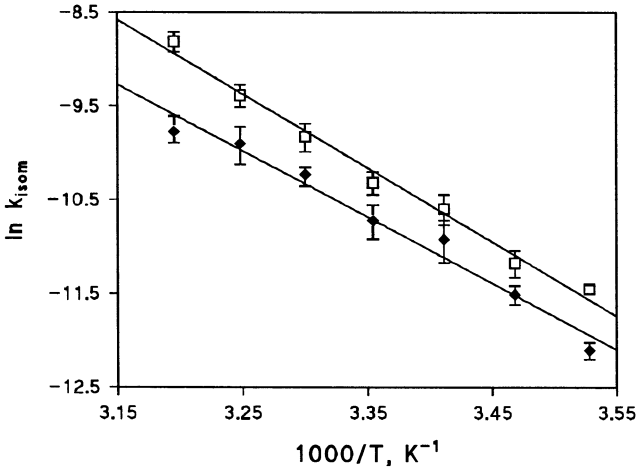

Figure 1. Plot of the temperature dependence of isomerization of **1** catalyzed by acetic acid (◆) and acetate ion (□). Error bars represent one standard deviation.

Table 2. Rate Constants for the Conversion of **1** to **2** Catalyzed by Acetate Ion[a]

temperature (°C)[b]	$10^3\,k_1^{OAc}(4\alpha)$ ($M^{-1}\,s^{-1}$)	$10^3\,k_1^{OAc}(4\beta)$ ($M^{-1}\,s^{-1}$)
12.8	0.73 ± 0.08	0.63 ± 0.11
19.2	1.33 ± 0.13	0.91 ± 0.18
25.5	1.7 ± 0.5	1.8 ± 0.2
32.9	4.8 ± 0.9	4.4 ± 0.7

[a] 3.3% MeOH, $\mu = 1.0$ M with NaCl. [b] Reported temperatures are ±0.2 °C.

The Arrhenius plots of $\ln k_1^{OAc}(4\alpha)$ and $\ln k_1^{OAc}(4\beta)$ are linear (Figure 2), with slopes corresponding to $\Delta H^{\ddagger} = 15 \pm 2$ kcal/mol and 16.4 ± 1.9 kcal/mol, respectively, and y-intercepts corresponding to $T\Delta S^{\ddagger} = -6 \pm 2$ and -5.0 ± 1.8 kcal/mol, respectively.

Temperature Dependence of the Rate Constant for Conversion of 2 to 1 (k_{-1}). Conversion of **2** to **1** was monitored by using sequential-mixing stopped flow, as previously described.[11] Dienolate ($\mathbf{2}^-$) is formed by rapidly mixing a solution of **1** with 0.1 M NaOH for ca. 0.5 s.[20] When this solution is quenched with acetate buffer, $\mathbf{2}^-$ is rapidly protonated to give **2**, which is then converted more slowly, almost exclusively, to **1**, resulting in a decrease in absorbance. The decay traces at 243 nm were fit to a first-order exponential decay to give the rate constants for acetate ion-catalyzed conversion of **2** to **1** at pH 3.9−5.1, ca. 7−41 °C. Since the rate of isomerization of **1**

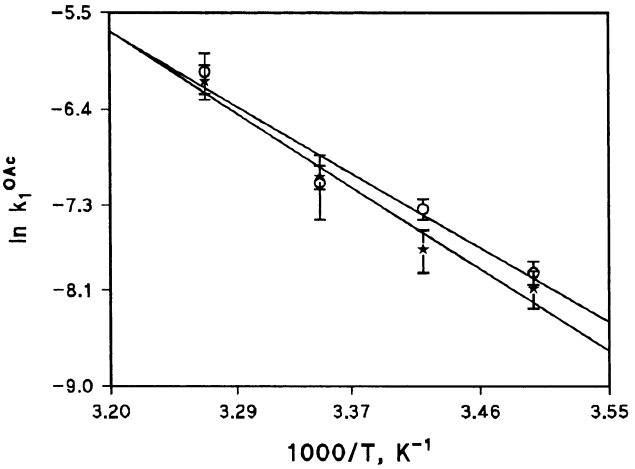

Figure 2. Plot of the temperature dependence of acetate ion-catalyzed proton abstraction of H-4α (○) and H-4β (★) from **1**. Error bars represent one standard deviation.

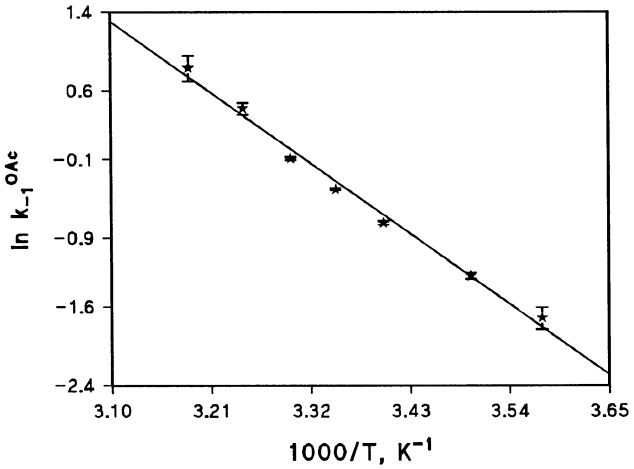

Figure 3. Plot of the temperature dependence of acetate ion-catalyzed protonation at C-4 of **2**. Error bars represent one standard deviation.

Table 3. Rate Constants for the Conversion of **2** to **1** Catalyzed by Acetate Ion[a]

temperature (°C)[b]	k_{-1}^{OAc} (M^{-1} s^{-1})
6.5	0.18 ± 0.02
12.8	0.276 ± 0.009
20.9	0.473 ± 0.010
25.5	0.668 ± 0.008
30.0	0.913 ± 0.013
34.9	1.52 ± 0.09
40.7	2.3 ± 0.3

[a] 3.3% MeOH, μ = 1.0 M with NaCl. [b] Reported temperatures are ±0.1 °C.

to **3** is much slower than the conversion of **2** to **1**, there is negligible interfering absorbance change due to conversion of **1** to **3**. Plots of the observed rate constants vs total acetate concentration are linear with no contribution from catalysis by HOAc. Table 3 lists these second-order rate constants (k_{-1}^{OAc}) at each temperature. Agreement with previously reported values at 25.0 °C[11] is excellent (±<5%). The Arrhenius plot of the natural logarithm of k_{-1}^{OAc} is linear (Figure 3), giving values of $\Delta H^{\ddagger}$ = 12.4 ± 0.5 kcal/mol and $T\Delta S^{\ddagger}$ = −5.2 ± 0.5 kcal/mol.

Temperature Dependence of the Rate Constant for the Conversion of 2 to 3 (k_2). Since partitioning of **2** in acetate buffer results almost exclusively in formation of **1** rather than **3** (e.g., $k_{-1} \gg k_2$), k_2 can be calculated from the equation $k_{isom} = k_1k_2/k_{-1}$. Calculations using the rate constants from the previous three sections show that conversion of **2** to **3** is catalyzed by both acetate ion (k_2^{OAc}) and acetic acid (k_2^{HOAc}) (Supporting Information, Table S1). The activation parameters for k_2^{OAc} are $\Delta H^{\ddagger}$ = 12.0 ± 1.8 kcal/mol and $T\Delta S^{\ddagger}$ = −8.4 ± 1.8 kcal/mol, and for k_2^{HOAc} they are $\Delta H^{\ddagger}$ = 10.3 ± 1.7 kcal/mol and $T\Delta S^{\ddagger}$ = −10 ± 2 kcal/mol.

Table 4. Rate Constants for Hydroxide-Catalyzed Interconversion of **1** and **2**$^-$[a]

temperature (°C)[b]	k_1^{OH} (M^{-1} s^{-1})	$k_{-1}^{H_2O}$ (s^{-1})
15.9	27.3 ± 0.1	1.17 ± 0.01
20.3	35.0 ± 0.2	1.89 ± 0.03
25.6	49.2 ± 0.7	2.90 ± 0.09
30.7	65.5 ± 1.3	4.51 ± 0.17
35.5	81.7 ± 0.6	7.40 ± 0.09
40.3	113 ± 3	10.6 ± 0.4

[a] 3.3% MeOH, μ = 1.0 M with NaCl. [b] Reported temperatures are ±0.1 °C.

Temperature Dependence of the Rate Constant for Hydroxide-Catalyzed Interconversion of 1 and 2$^-$. When **1** is mixed with relatively high concentrations of NaOH, the absorbance increases rapidly because of formation of **2**$^-$ and then more slowly as **2**$^-$ is converted into **3**.[20] To make formation of **3** invisible, the absorbance was monitored at or near 255 nm, the isosbestic point for **2**$^-$ and **3**. These traces were fit to a single exponential increase to give the observed pseudo-first-order rate constants for hydroxide-catalyzed deprotonation of **1**. Observed rate constants (an average of 6−10 runs) were plotted vs [HO$^-$] at each temperature (ca. 16−40 °C). The slopes of these lines are equal to the second-order rate constants for hydroxide-catalyzed proton abstraction from C-4 of **1** to form **2**$^-$ (k_1^{OH}), and the *y*-intercepts are equal to the rate constants for water-catalyzed protonation of **2**$^-$ at C-4 to give **1** ($k_{-1}^{H_2O}$) (Table 4). Values of $\Delta H^{\ddagger}$ and $T\Delta S^{\ddagger}$ for k_1^{OH} are 9.5 ± 0.2 and −5.7 ± 0.2 kcal/mol, respectively, and for $k_{-1}^{H_2O}$ the values are 16.3 ± 0.4 and −0.6 ± 0.4 kcal/mol, respectively.

Temperature Dependence of the Equilibrium Constants for Ionization of 1(K_a^1) and 2(K_a^2). The ionization constant for **1** (K_a^1) can be calculated from the experimentally determined rates for enolization (k_1^{OH}) and for reketonization ($k_{-1}^{H_2O}$), along with the value for the ion activity product constant of water (K_W). The natural logarithms of both k_1^{OH} and $k_{-1}^{H_2O}$ are linear with respect to inverse temperature (Figure 4) and can be used with the known temperature dependence of K_W[23] to calculate the temperature dependence of K_a^1 (Supporting Information, Table S2).

The value obtained for K_a^1 at 25.0 °C is (1.73 ± 0.10) × 10^{-13} M (pK_a^1 = 12.76), which is in excellent agreement with previously determined values.[20,24] In a similar manner, the ionization constant for **2** (K_a^2) can be calculated from the relationship $K_a^2 = K_a^1k_{-1}^{OAc}/k_1^{OAc}$ (Supporting Information, Table S2). The value obtained for K_a^2 at 25.0 °C is (3.0 ± 0.5) × 10^{-11} M (pK_a^2 = 10.5), which is in good agreement with the previously determined value.[11] Van't Hoff plots of K_a^1 and K_a^2 vs temperature yield the following enthalpies and entropies for

(23) Dean, J. A., Ed. *Lange's Handbook of Chemistry*, 13th ed.; McGraw-Hill: New York, 1985; pp 5−7.
(24) Pollack, R. M.; Zeng, B.; Mack, J. P. G.; Eldin, S. *J. Am. Chem. Soc.* **1989**, *111*, 6419.

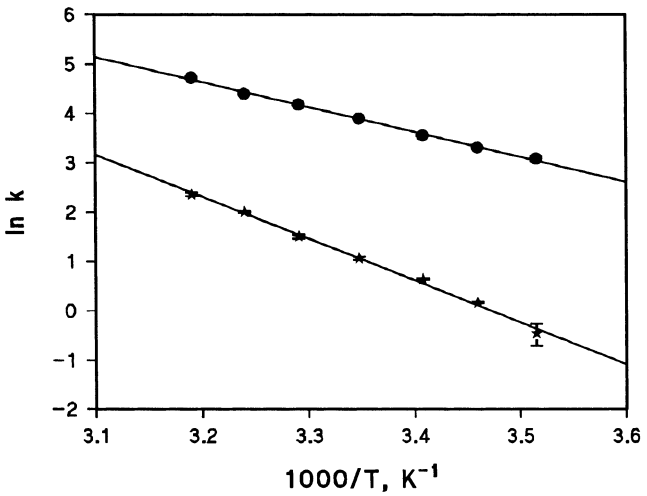

Figure 4. Plots of the temperature dependence of hydroxide-catalyzed proton abstraction from **1** (k_1^{OH}, ●) and water-catalyzed protonation at C-4 of $\mathbf{2}^-$ ($k_{-1}{}^{H_2O}$, ★). Error bars represent one standard deviation. Absence of error bars indicate that the error is less than the size of the symbol.

these ionizations: $\Delta H^\circ_{Ka}{}^1 = 7.8 \pm 0.4$ kcal/mol and $T\Delta S^\circ_{Ka}{}^1 = -9.6 \pm 0.5$ kcal/mol; $\Delta H^\circ_{Ka}{}^2 = 4.6 \pm 0.3$ kcal/mol and $T\Delta S^\circ_{Ka}{}^2 = -9.7 \pm 0.5$ kcal/mol (Table 6).

Discussion

Several factors determine the overall entropy change for second-order reactions between two molecules, A and B: (1) reorganization of the solvent molecules surrounding the reactants when A and B are brought together results in a positive $\Delta S^\ddagger$, (2) restriction of translational and rotational motion when A and B are brought together results in a negative $\Delta S^\ddagger$, and (3) other properties specific to A and B and the nature of the ensuing transition state may result in either a positive or negative $\Delta S^\ddagger$. For example, when neutral reactants form charged transition states, the entropy of activation is usually negative because of restriction of solvent molecules, whereas when charged reactants form uncharged (or less charged) transition states, the entropy of activation is usually positive because of the freeing up of solvent molecules.[25] Additionally, the formation of low-frequency vibrational levels often results in a positive change in entropy.[26−28] Bimolecular reactions generally result in a negative entropy of activation, which is predominantly due to the loss of translational and overall rotational motion.[26] Moore and Jencks compared an intermolecular nucleophilic attack of acetate on *p*-nitrophenylthioacetate to form acetic anhydride to the intramolecular reaction of *p*-nitrophenyl thiosuccinate to form succinic anhydride.[29] The intramolecular reaction has a more favorable entropy of activation by ca. 5 kcal/mol.[30] The authors attribute this entropy difference to the two reactants having already been brought together in the unimolecular reaction, thereby overcoming the negative entropy associated with that step.

The magnitude of activation entropies can vary because of the relative importance of the above factors. One notable example is the study by Vlasák and Mindl, who determined the enthalpies and entropies of activation for the alkaline hydrolysis of aryl carbazates.[31] Although values of $\Delta G^\ddagger$ for hydroxide-catalyzed hydrolysis of both phenylcarbazate and phenyl-2-methyl carbazate are similar ($\Delta G^\ddagger = 20.7$ and 22.1 kcal/mol, respectively), the difference in their entropies of activation is quite large ($T\Delta S^\ddagger = -0.6$ and -10.8 kcal/mol, respectively). The authors attribute this to a difference in the mechanism of hydrolysis for the two seemingly similar carbazates. Thus, phenylcarbazate undergoes an E1cB mechanism because of the loss of the ionizable proton on the nitrogen adjacent to the carbonyl group, whereas phenyl-2-methyl carbazate, which does not have an ionizable proton at that position, undergoes a $B_{Ac}2$ mechanism.

Table 5. Thermodynamic Activation Parameters for Interconversion of **1**, **2**, $\mathbf{2}^-$, and **3**

reaction	rate constant	$\Delta G^{\ddagger a}$ (kcal/mol)	$\Delta H^\ddagger$ (kcal/mol)	$T\Delta S^{\ddagger a}$ (kcal/mol)
$\mathbf{1} + {}^-OAc \rightarrow \mathbf{3}$	$k_{isom}{}^{OAc}$	23.5 ± 0.1	15.2 ± 0.8	-8.3 ± 0.8
$\mathbf{1} + HOAc \rightarrow \mathbf{3}$	$k_{isom}{}^{HOAc}$	23.7 ± 0.1	13.5 ± 0.8	-10.3 ± 1.0
$\mathbf{1} + {}^-OAc \rightarrow \mathbf{2}$	$k_1{}^{OAc}(4\alpha)$	21.1 ± 0.1	15 ± 2	-6 ± 2
	$k_1{}^{OAc}(4\beta)$	21.4 ± 0.1	16.4 ± 1.9	-5.0 ± 1.8
$\mathbf{2} + {}^-OAc \rightarrow \mathbf{1}$	$k_{-1}{}^{OAc}$	17.6 ± 0.1	12.4 ± 0.5	-5.2 ± 0.5
$\mathbf{2} + {}^-OAc \rightarrow \mathbf{3}$	$k_2{}^{OAc}$	20.4 ± 0.1	12.0 ± 1.8	-8.4 ± 1.8
$\mathbf{2} + HOAc \rightarrow \mathbf{3}$	$k_2{}^{HOAc}$	20.7 ± 0.1	10.3 ± 1.7	-10 ± 2
$\mathbf{1} + {}^-OH \rightarrow \mathbf{2}^-$	$k_1{}^{OH}$	15.1 ± 0.1	9.5 ± 0.2	-5.7 ± 0.2
$\mathbf{2}^- + H_2O \rightarrow \mathbf{1}$	$k_{-1}{}^{H_2O}$	16.8 ± 0.1	16.3 ± 0.4	-0.6 ± 0.4
$\mathbf{2}^- + HOAc \rightarrow \mathbf{3}$	$k_2{}^{HOAc}$	12.5 ± 0.1	8.4 ± 0.6	-4.2 ± 0.7
$\mathbf{2}^- + HOAc \rightarrow \mathbf{1}$	$k_{-1}{}^{HOAc}(4\alpha)$	10.1 ± 0.1	8.0 ± 1.7	-2.1 ± 1.2
	$k_{-1}{}^{HOAc}(4\beta)$	10.3 ± 0.1	9.6 ± 1.8	-0.7 ± 0.3

[a] Values given at 298 K.

Very little research has focused on activation enthalpies and entropies for enolizations. Chiang et al. have examined the temperature dependence of perchloric acid-catalyzed enolization of acetone and ketonization of its enol in both water and acetonitrile.[32] They found the entropies of activation for enolization of acetone to be similar in both water and acetonitrile ($T\Delta S^\ddagger = -3.6$ and -1.7 kcal/mol, respectively).[32] Additionally, the enthalpies of activation for this enolization are similar in both solvents ($\Delta H^\ddagger = 20.0$ and 20.2 kcal/mol, respectively). They compared the thermodynamic parameters for the keto−enol equilibrium in solution with those in the gas phase and found the values to be similar also. While these studies and others[29,31,33,34] have interpreted the thermodynamic activation parameters for relatively simple bimolecular processes, there have been no comprehensive studies of the temperature dependence of the microscopic rate constants for acid and base-catalyzed enolization/ketonization or isomerization.

Overall Isomerization of 1 to 3. Isomerization of **1** to **3** is catalyzed by both acetic acid and acetate ion. While $\Delta G^\ddagger$ for both processes is similar ($\Delta G^\ddagger_{HOAc} = 23.5 \pm 0.1$ kcal/mol and $\Delta G^\ddagger_{OAc} = 23.7 \pm 0.1$ kcal/mol), the enthalpies and entropies of activation differ slightly (Table 5). That is, while the enthalpy

(25) Carey, F. A.; Sundberg, R. J. *Advanced Organic Chemistry, Part A*: *Structure and Mechanisms*, 3rd ed.; Plenum: New York, 1990; p 196.
(26) Page, M. I.; Jencks, W. P. *Proc. Natl. Acad. Sci. U.S.A.* **1971**, *68*, 1678.
(27) Tidor, B.; Karplus, M. *J. Mol. Biol.* **1994**, *238*, 405.
(28) Villá, J.; Štrajbl, M.; Glennon, T. M.; Sham, Y. Y.; Chu, Z. T.; Warshel, A. *Proc. Natl. Acad. Sci. U.S.A.* **2000**, *97*, 11899.
(29) Moore, S. A.; Jencks, W. P. *J. Biol. Chem.* **1982**, *257*, 10882.
(30) Entropy (ΔS), as determined from eq 1, has units of cal/mol K. We report and discuss the entropic contribution to free energy ($T\Delta S$) in kcal/mol for comparison to ΔH and ΔG. Thus, a negative value for $T\Delta S$ is considered an entropy loss (entropic disadvantage), while a positive value for $T\Delta S$ is considered an entropy gain (entropic advantage).
(31) Vlasák, P.; Mindl, J. *J. Chem. Soc., Perkin Trans. 2* **1997**, 1401.
(32) Chiang, Y.; Kresge, A. J.; Schepp, N. P. *J. Am. Chem. Soc.* **1989**, *111*, 3977.
(33) Casale, J. F.; Lewin, A. H.; Bowen, J. P.; Carroll, F. I. *J. Org. Chem.* **1992**, *57*, 4906.
(34) Bowden, K.; Byrne, J. M. *J. Chem. Soc., Perkin Trans. 2* **1997**, 123.

Scheme 2

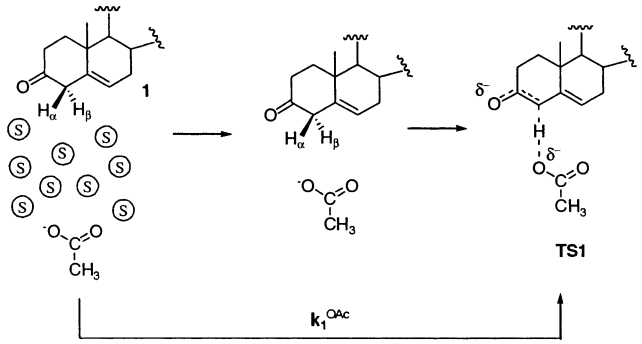

of activation is more favorable for the acid-catalyzed process, the entropy of activation is more favorable for the base-catalyzed process by ca. 2 kcal/mol. Since isomerization of **1** to **3** by acetate ion/acetic acid involves several steps and is pH dependent, it is necessary to determine the activation parameters for each of these steps, k_1, k_{-1}, and k_2, to make useful interpretations of the thermodynamic data.

Acetate Ion-Catalyzed Conversion of 1 to 2 (k_1^{OAc}). Although the overall isomerization is catalyzed by both acetic acid and acetate ion, catalysis of the initial step, proton abstraction from C-4, occurs only by acetate ion. Thus, the mechanism for formation of the dienol is most reasonably interpreted as a simple single-step proton abstraction from either C-4α or C-4β of the steroid. Both k_1^{OAc}(4α) and k_1^{OAc}(4β) have a relatively large enthalpic penalty ($\Delta H^{\ddagger}$ = ca. 16 kcal/mol) and a moderate entropic penalty ($T\Delta S^{\ddagger}$ = ca. −5 kcal/mol) (Table 5).

These values can be compared with those for methoxide-catalyzed proton abstraction from the α-carbon of ecgonine methyl ester ($\Delta H^{\ddagger}$ = 17 kcal/mol, $T\Delta S^{\ddagger}$ = −6.6 kcal/mol)[33] and nucleophilic attack of hydroxide on methyl *cis*-3-benzoyl-2,3-diphenylacrylate ($\Delta H^{\ddagger}$ = 13.8 kcal/mol, $T\Delta S^{\ddagger}$ = −6.0 kcal/mol).[34] Both of these reactions result in partial bond formation between a base or nucleophile with the reactant, and both result in the formation of a partial negative charge at the transition state. Similar enthalpies and entropies of activation are observed with acetate ion-catalyzed proton abstraction from **1**. As shown in Scheme 2, the transition state for k_1^{OAc} (**TS1**) involves (1) partial bond formation between acetate ion and either the α or β proton and (2) formation of an incipient carbanion at C-4 whose negative charge is delocalized onto O-3 of the carbonyl. A negative entropy for deprotonation at either C-4α or C-4β is not unexpected, as this step requires bringing two molecules together (loss of entropy), followed by partial bond formation, which results in low-frequency vibrations (small gain of entropy).[26,28] The activation parameters of acetate-catalyzed proton abstraction (k_1^{OAc}) can also be compared to proton abstraction by hydroxide ion (k_1^{OH}). The activation entropies for both reactions are experimentally indistinguishable (Table 5). The relative base strengths, though, are evidenced in the lower heat of activation ($\Delta\Delta H^{\ddagger}$ ca. −6 kcal/mol) for the hydroxide ion reaction.

Partitioning of the Intermediate Dienol (2) (k_{-1} and k_2). Acetic Acid-Catalyzed Conversion of 2 to 3 (k_2^{HOAc}). Protonation of **2** at C-6 (k_2) is catalyzed by both acetate ion (k_2^{OAc}) and acetic acid (k_2^{HOAc}). The acetic acid-catalyzed conversion (k_2^{HOAc}) is most simply interpreted as direct protonation of **2** (dienol) by acetic acid.[11] The corresponding activation enthalpy for this step is 10.3 kcal/mol (Table 5), which is similar to that for protonation of acetone enol by perchloric acid ($\Delta H^{\ddagger}$ = 9.7 kcal/mol).[32] The entropy of activation for k_2^{HOAc} is quite large and negative ($T\Delta S^{\ddagger}$ = −10 kcal/mol). Similar to k_1^{OAc}, bringing two reactants together is expected to result in a negative entropy. For k_2^{HOAc}, however (as shown in Scheme 3), there is an additional entropy loss during proton transfer due to the development of two new partial charges from previously neutral dienol. The partial positive on the enol oxygen of **2** and the partial negative on the acetic acid oxygen are expected to restrict solvent molecules at the transition state, leading to a more negative entropy of activation for k_2^{HOAc} than k_1^{OAc}.

Table 6. Thermodynamic Equilibrium Parameters for Interconversion of **1**, **2**, and **2**$^-$

reaction	equilibrium constant	$\Delta G^{\circ a}$ (kcal/mol)	ΔH° (kcal/mol)	$T\Delta S^{\circ a}$ (kcal/mol)
1 ⇌ **2**$^-$ + H$^+$	K_a^1	17.4 ± 0.1	7.8 ± 0.4	−9.6 ± 0.5
2 ⇌ **2**$^-$ + H$^+$	K_a^2	14.5 ± 0.1	4.6 ± 0.3	−9.7 ± 0.5
2 + −OAc ⇌ **2**$^-$ + HOAc	K_{eq}	7.9 ± 0.1	3.6 ± 0.2	−4.2 ± 0.7
1 ⇌ **2**	K_{ext}	2.9 ± 0.1	3.2 ± 0.4	0.1 ± 0.5

[a] Values given at 298 K.

Scheme 3

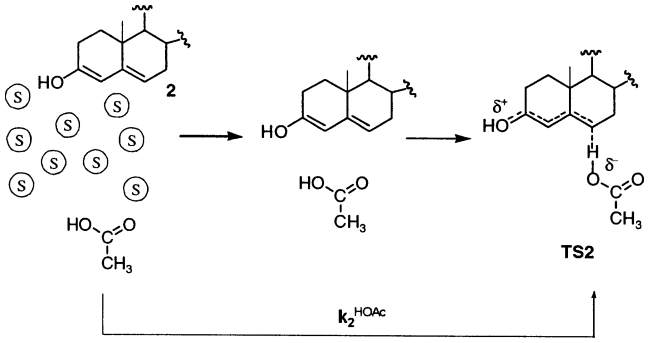

Scheme 4

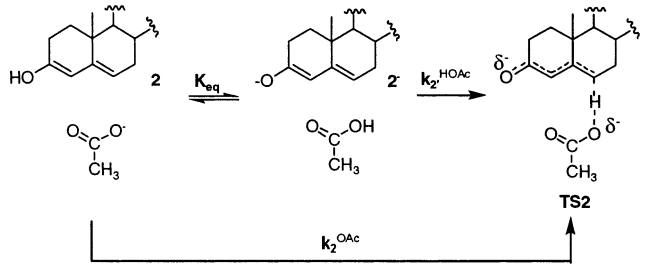

Acetate Ion-Catalyzed Conversion of 2 to 3 (k_2^{OAc}). The mechanism for acetate ion-catalyzed conversion of **2** to **3** (k_2^{OAc}) can be broken down into two steps as shown in Scheme 4.

The first step is a rapid equilibrium between acetate ion/dienol and acetic acid/dienolate (K_{eq}), and the second step involves proton transfer from acetic acid to the dienolate at C-6 ($k_2'^{HOAc}$). The equilibrium constant for the first step is the ratio of the ionization constants for **2** and acetic acid ($K_{eq} = K_a^2/K_a^{HOAc}$). K_{eq} was calculated over a range of temperatures (Supporting Information, Table S3) from the temperature dependence of K_a^2 (Table 6) and the temperature independence of K_a^{HOAc} over the range studied here ($K_a^{HOAc} = 1.75 \times 10^{-5}$ M[23]). The activation parameters for this equilibrium are ΔH_{Keq} = 3.6 kcal/mol and $T\Delta S_{Keq}$ = −4.2 kcal/mol (Table 6). The magnitude of $k_2'^{HOAc}$ at various temperatures was calculated from the equation $k_2'^{HOAc} = k_2^{OAc}/K_{eq}$ (Supporting Information, Table S3). From these results, protonation of **2**$^-$ at C-6 by acetic acid ($k_2'^{HOAc}$) has an

Scheme 5

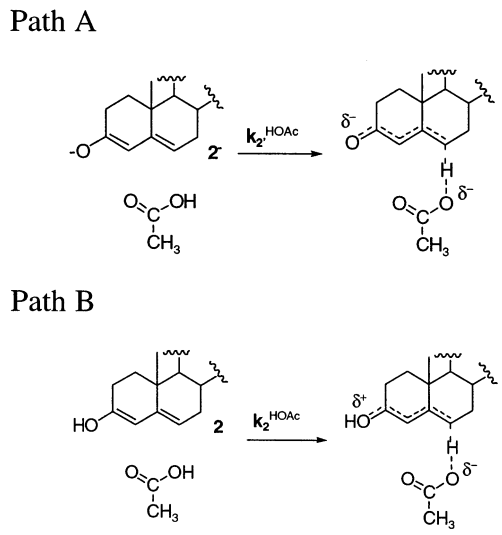

activation enthalpy and an activation entropy of 8.4 and −4.2 kcal/mol, respectively (Table 5).

Comparison of the activation parameters for acetic acid-catalyzed protonation of **2** (k_2^{HOAc}) and of $\mathbf{2}^-$ ($k_{2'}^{HOAc}$) indicates that the enthalpies for both processes are similar within error. However, the entropy loss for protonation of **2** is ca. 6 kcal/mol larger than the entropy loss for protonation of $\mathbf{2}^-$. Both processes involve diffusion and orientation of the reacting molecules, which results in a negative activation entropy. Interestingly, the entropy loss for $k_{2'}^{HOAc}$ is similar to that for k_1^{OAc}. As shown in Scheme 5 (Path A) there is little to no net change in charge in going from the ground-state reactants to the transition state for protonation of the dienolate ($k_{2'}^{HOAc}$). The same is true for k_1^{OAc} (Scheme 2). Conversely, for protonation of the dienol (k_2^{HOAc}, Scheme 5, Path B) at the transition state, positive charge is developing on the previously neutral ground-state dienol, and negative charge is developing on the previously neutral ground-state acid, restricting solvent molecules that are hydrogen bonded to it. The result is a more negative entropy of activation for k_2^{HOAc} (Path B) than for $k_{2'}^{HOAc}$ (Path A).

Acetate Ion-Catalyzed Conversion of 2 to 1 (k_{-1}^{OAc}). Similar to k_2^{OAc}, k_{-1}^{OAc} can be broken down into two steps: equilibrium conversion of the dienol (**2**) to the dienolate ($\mathbf{2}^-$), followed by protonation of $\mathbf{2}^-$ at C-4 by acetic acid ($k_{-1'}^{HOAc}$) (Scheme 6), with $k_{-1'}^{HOAc} = k_{-1}^{OAc}/K_{eq}$.

Because $k_{-1}^{OAc}/K_a^2 = k_1^{OAc}/K_a^1$, it follows that $k_{-1'}^{HOAc} = k_1^{OAc}K_a^{HOAc}/K_a^1$. Since $k_1^{OAc} = k_1^{OAc}(4\alpha) + k_1^{OAc}(4\beta)$, $k_{-1'}^{HOAc}$ can be calculated for both the 4α and 4β protons ($k_{-1'}^{HOAc}(4\alpha)$ and $k_{-1'}^{HOAc}(4\beta)$) (Supporting Information, Table S3). Activation enthalpies and entropies for both $k_{-1'}^{HOAc}(4\alpha)$ and $k_{-1'}^{HOAc}(4\beta)$ are given in Table 5.

Scheme 6

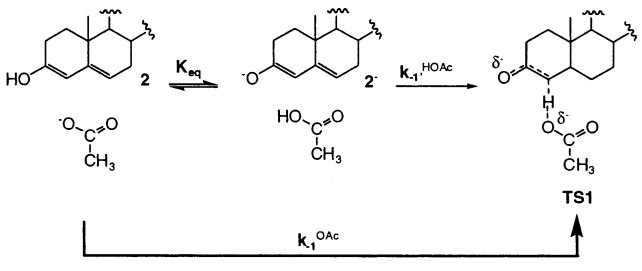

Scheme 7

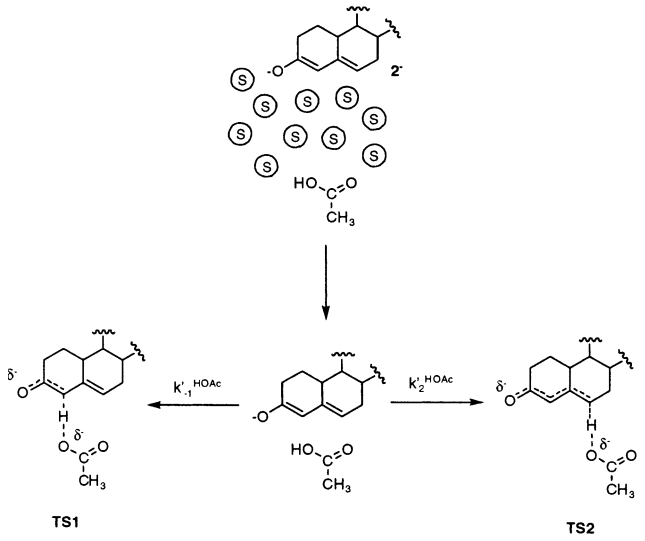

As shown previously,[11] protonation of $\mathbf{2}^-$ at C-4α is competitive with protonation at C-4β. In contrast, protonation at C-6α is ca. 100-fold slower than at C-6β.[24] The difference in $\Delta G^{\ddagger}$ between protonation of dienolate ($\mathbf{2}^-$) at C-6β and C-4 (α or β) is ca. 2 kcal/mol (Scheme 7). Although the relatively high experimental errors in the calculated values of $\Delta H^{\ddagger}$ and $T\Delta S^{\ddagger}$ for these rate constants limit the interpretation of these parameters, it is of interest to note that the 100-fold increase in the rate of protonation at C-4β relative to C-6β is a result of the difference in the entropies of activation. $T\Delta S^{\ddagger}$ for $k_{2'}^{HOAc}$ is significantly less favorable than for $k_{-1'}^{HOAc}(4\beta)$ ($T\Delta\Delta S^{\ddagger}$ ca. −3 kcal/mol).

Interconversion of 1 and 2: The Keto−Enol Equilibrium Constant (K_{ext}). Finally, knowledge of the enthalpy and entropy for the acid dissociation constants for **1** (K_a^1) and **2** (K_a^2) (Table 6) allows a calculation of the enthalpy and entropy associated with the keto−enol equilibrium (K_{ext}) and a completion of the thermodynamic cycle (Scheme 8). Ionization of both **1** (K_a^1) and **2** (K_a^2) to form $\mathbf{2}^-$ results in a large entropic penalty ($T\Delta S_{Ka}^1 = -9.6$ kcal/mol and $T\Delta S_{Ka}^2 = -9.7$ kcal/mol), which is likely due to restriction of free solvent molecules that stabilize the negative charge that has been formed on O-3 of the steroid. In each case, the enthalpy of ionization is also unfavorable ($\Delta H_{Ka}^1 = 7.8$ kcal/mol and $\Delta H_{Ka}^2 = 4.6$ kcal/mol). These results lead to a calculated entropy for the keto−enol equilibrium between **1** and **2** ($T\Delta S_{Kext}$) of ca. 0 kcal/mol. Comparison of the structures in Scheme 8 shows that while **2** has an additional bond with

Scheme 8

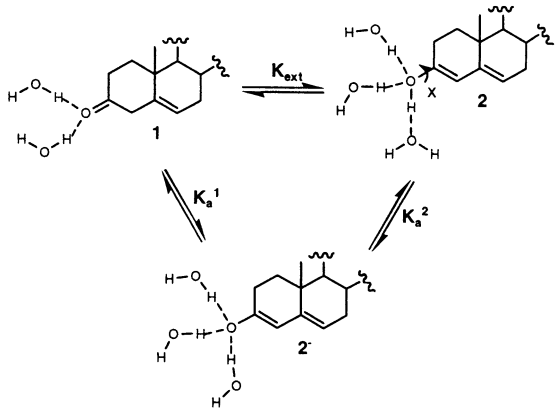

free rotation that **1** does not (denoted x on **2** in Scheme 8) ($\Delta S > 0$ for K_{ext}), **2** is expected to restrict three solvent molecules, whereas **1** will restrict two ($\Delta S < 0$ for K_{ext}). These entropy terms apparently cancel out, giving $\Delta S = 0$ for this equilibrium. The keto−enol enthalpy ($\Delta H_{Kext} = 3$ kcal/mol) entirely determines the free energy for the keto−enol equilibrium.

Relevance to the Mechanism of Action of KSI. Since acetate serves as a good model for the active-site base in KSI (Asp38), a comparison of the activation parameters for the enzymatic and the nonenzymatic reactions should shed light on the catalytic strategy of KSI. A determination of the free-energy profiles for both the acetate- and KSI-catalyzed reactions[10] has shown that KSI stabilizes the intermediate dienolate relative to solution by ca. 11 kcal/mol, leading to an internal equilibrium constant at the active site of about unity,[10] consistent with the expectation for an ideal or "perfect" enzyme.[35] In addition, KSI stabilizes both the enolization and ketonization transition states (**TS1** and **TS2**, respectively) by >10 kcal/mol.

The differences between the enzymatic active site of KSI and the aqueous solution in which the acetate experiments were performed enable one to hypothesize what results might be expected for the activation enthalpy and entropy of the corresponding chemical steps on the enzyme. The hydrophobic active site of KSI contains two hydrogen bond donors (Tyr14 and Asp99) oriented to stabilize the negative charge on the dienolate intermediate and the flanking transition states.[36] Are these effects predominantly enthalpic or entropic? In preliminary experiments, the temperature dependence of k_{cat}/K_M for the D38E mutant of KSI indicates that, relative to acetate-catalyzed isomerization, the enthalpy of activation for the isomerization of **1** to **3** is significantly lowered and the entropy of activation is significantly increased, both of these effects serving to lower $\Delta G^{\ddagger}$ for the isomerization reaction (unpublished results). These results follow the general trend that enzymes lower $\Delta H^{\ddagger}$ and raise $T\Delta S^{\ddagger}$, which is seen when enzyme reactions are compared to their nonenzymatic counterparts.[37]

Previous characterization of the free-energy profile for D38E catalysis indicates that the two chemical transition states are of about equal energy,[10] whereas for acetate catalysis, these transition states differ by ca. 2 kcal/mol.[11] Since the difference between **TS1**and **TS2** for acetate catalysis appears primarily in the entropy term, it will be interesting to see whether D38E equalizes the entropic penalties of both transition states to make them equal in free energy, or whether the effect is enthalpic. These experiments are underway in our laboratory.

Materials and Methods

Materials. 5-Androstene-3,17-dione was prepared by G. Blotny of this laboratory according to a previously published procedure.[24] Deuterated solvents and reagents were ≥99% atom. Acetate buffers and hydroxide solutions were prepared with reagent-grade chemicals or better. Buffer pH was determined on a Radiometer PHM85 Precision pH meter and is within 0.1 unit of the values given throughout the text.

Determination of the Overall and Microscopic Rate Constants for Acetate-Catalyzed Isomerization. The overall isomerization rate constant, k_{isom}, and the microscopic rate constants, k_1, k_{-1}, and k_2, were determined as described previously[11] over the temperature range of ca. 5−40 °C with modifications as described below. For all regression fitting, Figure P software was used.

Determination of the Rate Constant for Overall Isomerization of 1 to 3 (k_{isom}). Overall isomerization of **1** by AcOH/AcO$^-$ (k_{isom}) was monitored on a Varian Cary 100 Bio spectrophotometer at 248 nm and 10.3−39.8 °C in ca. 5° increments (λ_{max} for **3** is 248 nm and does not vary significantly over the temperature range studied). Acetate buffers were thermostated at each temperature for at least 15 min and an additional 2 min after addition of **1**, before commencing a run (conditions in cuvette: [**1**] ∼50 μM, [AcO$^-$]/[AcOH] = 0.19−5.8, [AcO$^-$ + AcOH] = 0.227−3.98 M, μ = 1.0 M with NaCl, 3.3% MeOH). At each temperature, progress curves were monitored for 4−5 half-lives.

Determination of the Rate Constant for Conversion of 1 to 2 (k_1). Proton exchange with deuterium at C-4 (k_1) was determined in D_2O on a Bruker Avance 500 MHz NMR spectrometer at 12.8−32.9 °C in ca. 7° increments. Deuterated acetate buffers were prepared by adding the appropriate amount of NaOD to AcOD/D_2O solutions to yield the desired acetate ion/acetic acid ratio. These solutions were thermostated in the spectrometer for at least 15 min prior to addition of **1**. Then sample tubes were ejected, and 20 μL of a stock solution of **1** in MeOD was added (conditions in tube: [**1**] ∼100 μM, [AcO$^-$]/[AcOD] = 0.25−2.5, [AcO$^-$] = 0.0221−0.400 M, μ = 1.0 M with NaCl, 3.3% MeOD). The reaction mixture was thermally equilibrated for an additional 5−10 min before commencing a run. Disappearance of both the 4α and 4β protons was monitored at 2.82 and 3.45 ppm, respectively, for 3−4 half-lives.

Determination of the Rate Constant for Conversion of 2 to 1 (k_{-1}). The rate constant for protonation of **2** at C-4 by acetate (k_{-1}) was determined using a Hi-Tech PQ/SF-53 double-mixing stopped-flow spectrophotometer at or near 243 nm and 6.5 − 40.7 °C in ca. 5° increments (the isosbestic point for **2** and **3** varies slightly over the temperature range studied), similar to a method used previously in our laboratory.[11] All solutions were thermostated to reach the desired temperature for at least 15 min prior to mixing. A solution of **1** (ca. 500 μM) in 70% MeOH was mixed with a 0.1 M solution of NaOH in a 1:1 ratio and allowed to react for 0.5 s, thereby generating **2**$^-$. The resulting solution was quenched with various acetate buffers in a 1:10 ratio to produce **2** (conditions in the observation cell: [**2**] ∼50 μM, [AcO$^-$]/[AcOH] = 0.10−2.9, [AcO$^-$ + AcOH] = 0.269−1.82 M, μ = 1.0 M with NaCl, 3.3% MeOH). The pseudo-first-order decay of **2** to **1** was monitored for 5−7 half-lives.

Determination of the Rate Constants for Hydroxide-Catalyzed Interconversion of 1 and 2$^-$. The rate constants for proton abstraction from C-4 of **1** by hydroxide (k_1^{OH}) and reprotonation at C-4 of **2**$^-$ by H_2O ($k_{-1}^{H_2O}$) were determined on a Hi-Tech SF-61 DX2 double-mixing stopped-flow spectrophotometer at or near 255 nm and 15.9−40.3 °C in ca. 5° increments (λ_{max} for **2**$^-$ varies slightly over the temperature range studied), according to a previous procedure.[20] All solutions were thermostated for at least 15 min to reach the desired temperature prior to commencing a run. A solution of **1** in 6.6% MeOH was rapidly mixed with various concentrations of NaOH in a 1:1 ratio (conditions in observation cell: [**1**] ∼30 μM, [HO$^-$] = 0.0500−0.200 M, μ = 1.0 M with NaCl, 3.3% MeOH). The increase in absorbance due to formation of **2**$^-$ was monitored for 5−7 half-lives.

Acknowledgment. This research was supported by a grant from the National Institutes of Health (GM 31885). We thank G. Blotny of this laboratory for the gift of 5-androstene-3,17-dione.

Supporting Information Available: Tables of the calculated rate constants k_2^{HOAc}, k_2^{OAc}, $k_{-1}{}^{HOAc}(4\alpha)$, and $k_{-1}{}^{HOAc}(4\beta)$ and of the calculated equilibrium constants K_a^1, K_a^2, and K_{eq} (PDF). This information is available free of charge via the Internet at http://pubs.acs.org.

JA035957R

(35) Albery, J. W.; Knowles, J. R. *Biochemistry* **1976**, *15*, 5613.
(36) Wu, Z. R.; Ebrahimian, S.; Zawrotny, M. E.; Thornburg, L. D.; Perez-Alvarado, G. C.; Brothers, P.; Pollack, R. M.; Summers, M. F. *Science* **1997**, *276*, 415.
(37) Wolfenden, R.; Snider, M.; Ridgeway, C.; Miller, B. *J. Am. Chem. Soc.* **1999**, *121*, 7419.